Indian J. Phys. 73A (1), 73–89 (1999)

IJP A
— an international journal

QCD physics at Tevatron

M R Krishnaswamy

Tata Institute of Fundamental Research, Homi Bhabha Road,
Colaba, Bombay-400 005, India

Abstract : The success of Quantum Chromodynamics (QCD) in explaining many of the experimental results at high energies has prompted experimentalists to undertake high precision tests of the strong interaction at the Tevatron p-pbar Collider ($\sqrt{s}$ = 1.8 TeV) in Fermilab. CDF and D0 exprimental groups have recorded data with integrated luminosities of over 100 pb^{-1} at this collider facility. The data with final states of jets, direct photon or W are a rich ground of 'testing' the QCD predictions. Upto now strong interaction studies in jet physics at hadron colliders have been rather haphazard. One compares a given distribution with the theory *i.e.* a Next to Leading Order (NLO) perturbative QCD prediction utilizing α_s and Parton Density Functions (PDF) mainly from expeiments at low Q^2. If there is agreement, one tries to learn from the agreement. If there is disagreement one tries to adjust the PDFs. With the present sets of large data it is possible to reduce the choice in different PDFs and to look for higher order effects.

In this brief survey of QCD results from Tevatron, only the major issues are addressed. Table 1 shows the experimental 'definition' of various final states for $\sqrt{s}$ = 1.8 TeV. These definitions are followed throughout unless specified otherwise in individual cases.

Keywords : QCD, Tevatron, jet

PACS Nos. : 12.38.-t, 13.87.-a

1. Inclusive jet production

The measurement of the inclusive jet cross section is a simple but fundamental test of QCD. High transverse momentum jets are predominantly produced in p-pbar collisions by two body scattering of a single proton constituent with an antiproton constituent. Such events typically produce a pair of back-to-back jets (clusters of particles), each resulting from the fragmentation of a final state quark or gluon. Next-to-leading order (NLO) calculations upto $O(\alpha_s^3)$ level [1,2] include the possibility of a third radiated parton reducing the theoretical uncertainties to 10–20%.

Table 1. Identification of particles in CDF, D0 experiments at Tevatron.

Particle	Method	Cuts
Jets	Fixed cone algorithm	$\Delta\sqrt{(\Delta\eta^2 + \Delta\phi^2)} = 0.7$ $E_T > \sim 15$ GeV
Photons	Isolated EM cluster	$E_T > \sim 12$ GeV
Electrons	Isolated EM cluster with matching track	$E_T > \sim 12$ GeV
W	Isolated EM cluster	E_T (lepton) $> \sim 20$ GeV $\not{E} > 20 \sim 25$ GeV

(i) Cross section data ($d\sigma/dE_T$):

The inclusive jet cross section is defined as

$$\frac{d\sigma}{dE_T} = \int d\eta \frac{d^2\sigma}{dE_T d\eta} = \frac{1}{L}\frac{N_{\text{jet}}}{\Delta E_T},$$

where L is the integrated luminosity, and N is the number of jets in a bin of ΔE_T. The measured E_T spectrum is corrected for detector and smearing effects caused by finite E_T resolution.

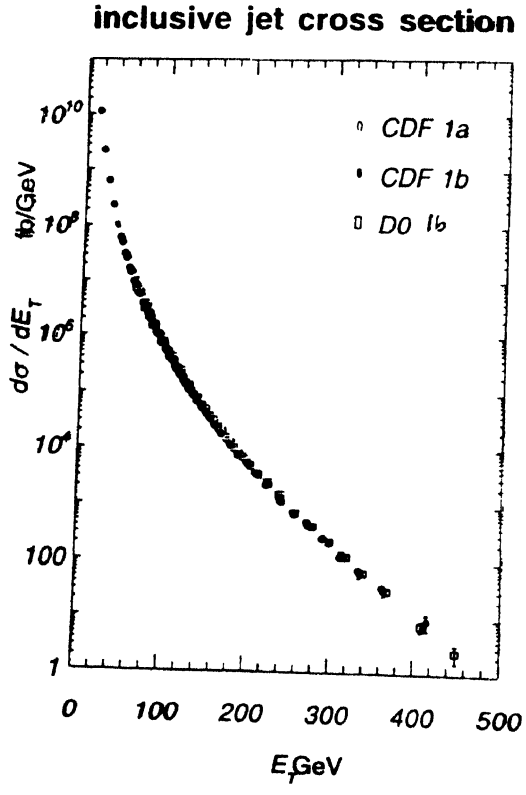

Figure 1. The CDF (Run 1a & 1b) and D0 (Run 1b) inclusive jet cross section as a function of E_T

The inclusive jet cross section ($d\sigma/dE_T$) is shown as a function of transverse energy E_T in Figure 1. In order to bring out the salient features, the cross section [3–6] is

multiplied by E_T [7] and shown in Figures 2 and 3 for CDF and D0. The D0 ($|\eta| < 0.5$) data have to be rapidity-adjusted to match the rapidity range of the CDF data ($0.1 < |\eta| < 0.7$) for comparison. The effect of this rapidity adjustment of D0 data is shown separately in

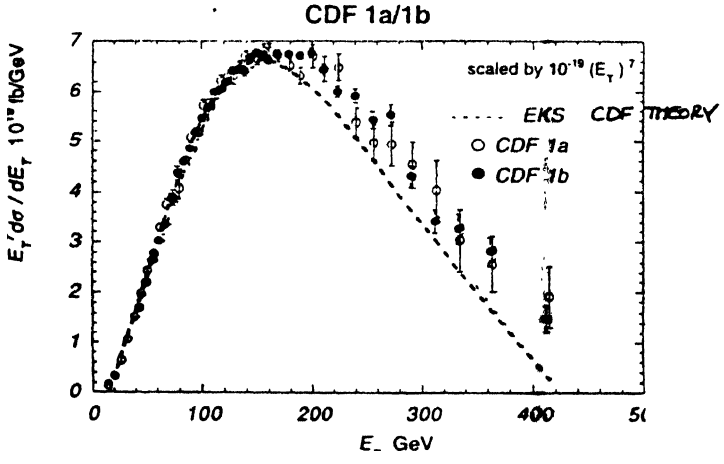

Figure 2. The CDF inclusive jet cross section multiplied by E^7 as a function of E_T. The dashed line is the prediction from Ellis *et al* [2].

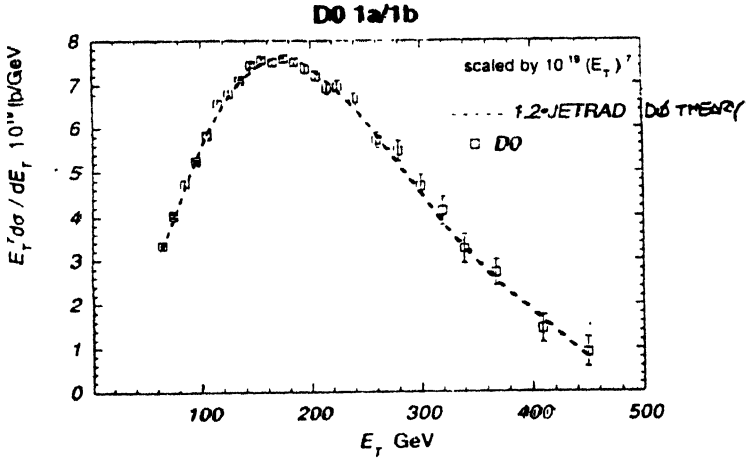

Figure 3. The D0 inclusive jet cross section multiplied by E^7 as a function of E_T. The dashed line is the prediction of JETRAD model of Giele *et al* [1] multiplied by 1.20.

Figure 4. From the comparison of CDF and D0 data (after rapidity-adjustment) shown in Figure 5 one can clearly see that in the region of 120 to 220 GeV of E_T there is clearly a disagreement between these two experiments. However, whereas CDF reports a disagreement between their data and Ellis *et al* [2] calculation above 160 GeV, the D0 data agrees well with the JETRAD calculation of Giele *et al* [1] after an overall multiplication of the calculated values by 1.2. Thus, both in individual experimental values and in theory in the high E_T region there are questions to be resolved. It may be pointed out that both D0 and

CDF quote 4–5% normalization uncertainty due to luminosity. Systematic uncertainties in the inclusive jet cross section amounts to 20% for CDF and 30% for D0.

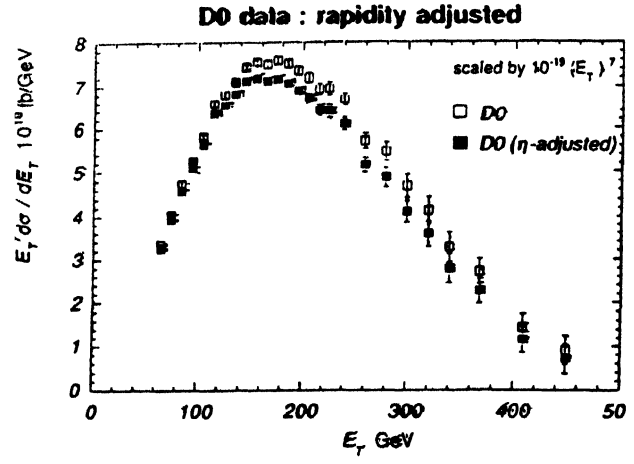

Figure 4. The effect of rapidity-adjustment on D0 data. The data has been adjusted to match with the rapidity region of CDF data.

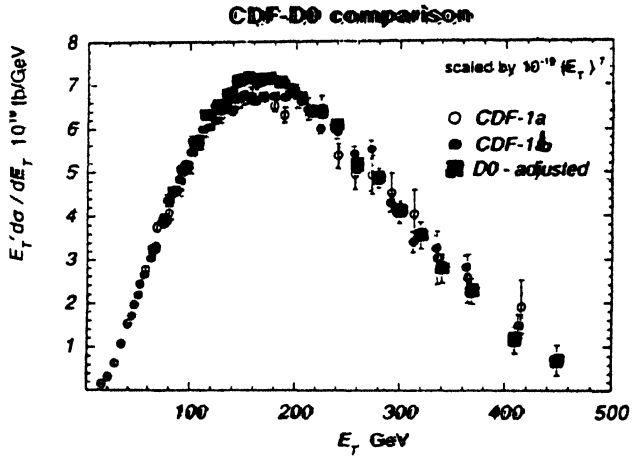

Figure 5. The CDF and D0 data comparison. Note that the D0 data have been rapidity-adjusted to enable the comparison.

(ii) Significance :

The deviation from theory of the CDF data at high E_T may be the effect of the Ellis *et al* model. It may be noted that even the D0 data requires normalization to match the JETRAD model. Thus, models are sufficiently different to complicate things since by using different PDFs they introduce moderate to significant dependence of cross section on E_T. This dependence is brought out in Figure 6 where the ratio of the cross sections obtained in JETRAD calculation using two different PDFs (CTEQ2M and MRSD0) are plotted as a

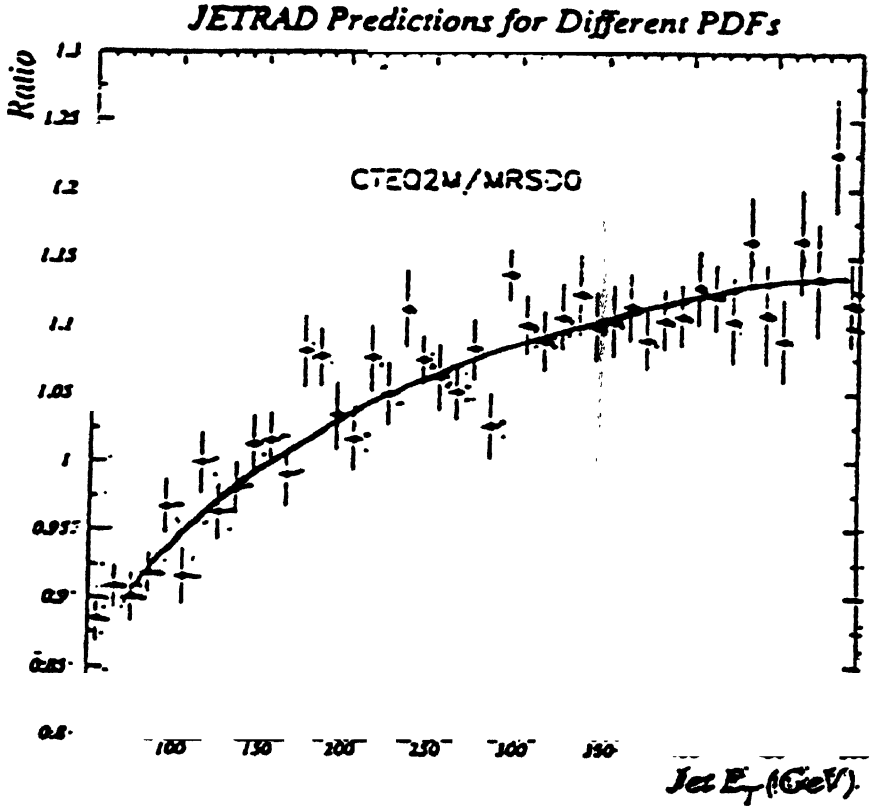

Figure 6. The effect of different PDFs in a model. The ratio of the predictions of JETRAD model using CTEQ2M and MRSD0 PDFs as a function of jet E_T.

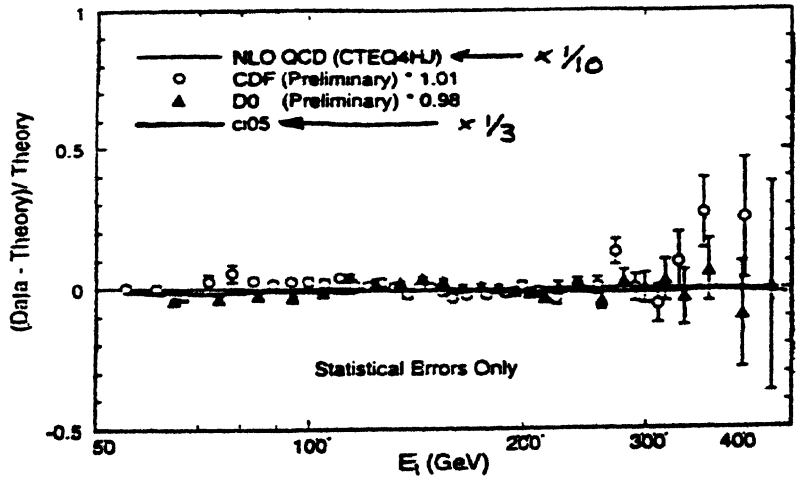

Figure 7. The CDF and D0 data have been deliberately modified for PDF effects to get 'fake data'. The ratio (data-theory)/theory for this 'fake data' is plotted as a function of E_T to show that PDFs are important. The overall agreement of 'fake data' after modification with NLO QCD model using CTEQ4HJ PDF may be noted.

function of Jet E_T. A preliminary "exercise' by Brock [7] shows that models perhaps represent a systematic uncertainty in simulating physics and if one considers the effect of different models, different cone radii for jet selection *etc.* one may possibly account for the difference between the CDF data and Ellis *et al* model beyond about 200 GeV. An example of deliberately modifying (preliminary) data and theory and then comparing is shown in Figure 7. The final agreement between the 'fake data' and model using CTEQ4HJ PDF is quite good. An additional conclusion is that the gluon PDF (not well measured) may be important for the calculation since even at moderate E_T the cross section is sensitive to the gluon distribution. The difference in data between the two experiments in a small region of E_T is more difficult to understand. It is too premature to say that the correction due to rapidity adjustment of D0 data is not enough in this region since the systematic errors are large. This requires further study.

2. Dijet events

(i) Rapidity gaps and hard colour-singlet exchange :

Rapidity gaps, namely regions of rapidity containing no final-state particles, are expected to occur between jets when a colour-singlet is exchanged between the interacting hard partons.

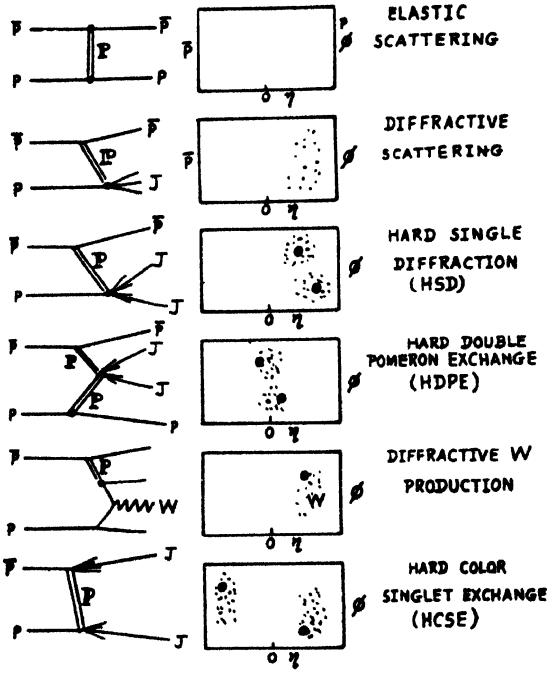

Figure 8. Event topologies arising in different types of POMERON exchange. The large rapidity gap resulting from the Hard Colour-singlet exchange is conspicuous.

The exchange of a photon, W boson, Z boson or a hard QCD Pomeron is expected to give such an event topology. The different event topologies arising out of different types of scattering are shown in Figure 8. The large rapidity gap due to the exchange of a hard colour-singlet is the motivation for this study.

Rapidity gaps will not be observed in the final state if spectator interactions produce particles between the jets. Approximately 10–30% of rapidity gap events are expected to survive spectator interactions [8,9] and roughly 1–3% of jet events are expected to have an observable rapidity gap between the jets from Pomeron exchange.

It is not possible to distinguish colour-singlet rapidity gaps from those that occur in colour-octet exchange on an event by event basis. But differences in the particle multiplicity distributions can be used to search for a colour-singlet signal. Experimentally, both D0 and CDF measure the multiplicity of particles in the pseudorapidity interval $\left(\Delta\eta_c = |\eta_1 - \eta_2| - 2R,\right.$ where the cone radius $\left.R = \sqrt{\Delta\eta^2 + \Delta\phi^2}\right)$.

The CDF data on diffractive and non-diffractive scattering for different rapidity regions (as defined by different detector components) are shown in Figure 9. It can clearly

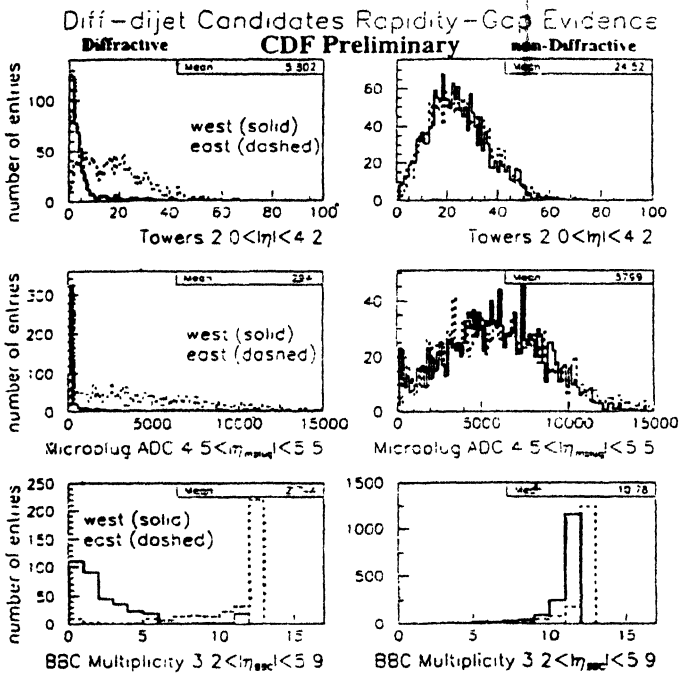

Figure 9. The CDF evidence for rapidity gaps. The diagrams on the left show the diffractive interaction results in different rapidity regions where the difference in the distribution in the east and west side can clearly be seen. The right hand diagrams belonging to the non-diffractive interactions in the same rapidity regions show no rapidity gap in the distributions.

be seen that in the case of diffractive scattering the events corresponding to east and west sides (*i.e.* different η's) the distributions are different and these contain rapidity gap events. The non-diffractive distributions corresponding to the same η regions do not show any significant difference in the distributions.

Lego plots of deposited energy in the $\phi - \eta$ plane of some events observed in D0 with different event topologies are shown in Figure 10. The rapidity gap in the case of event

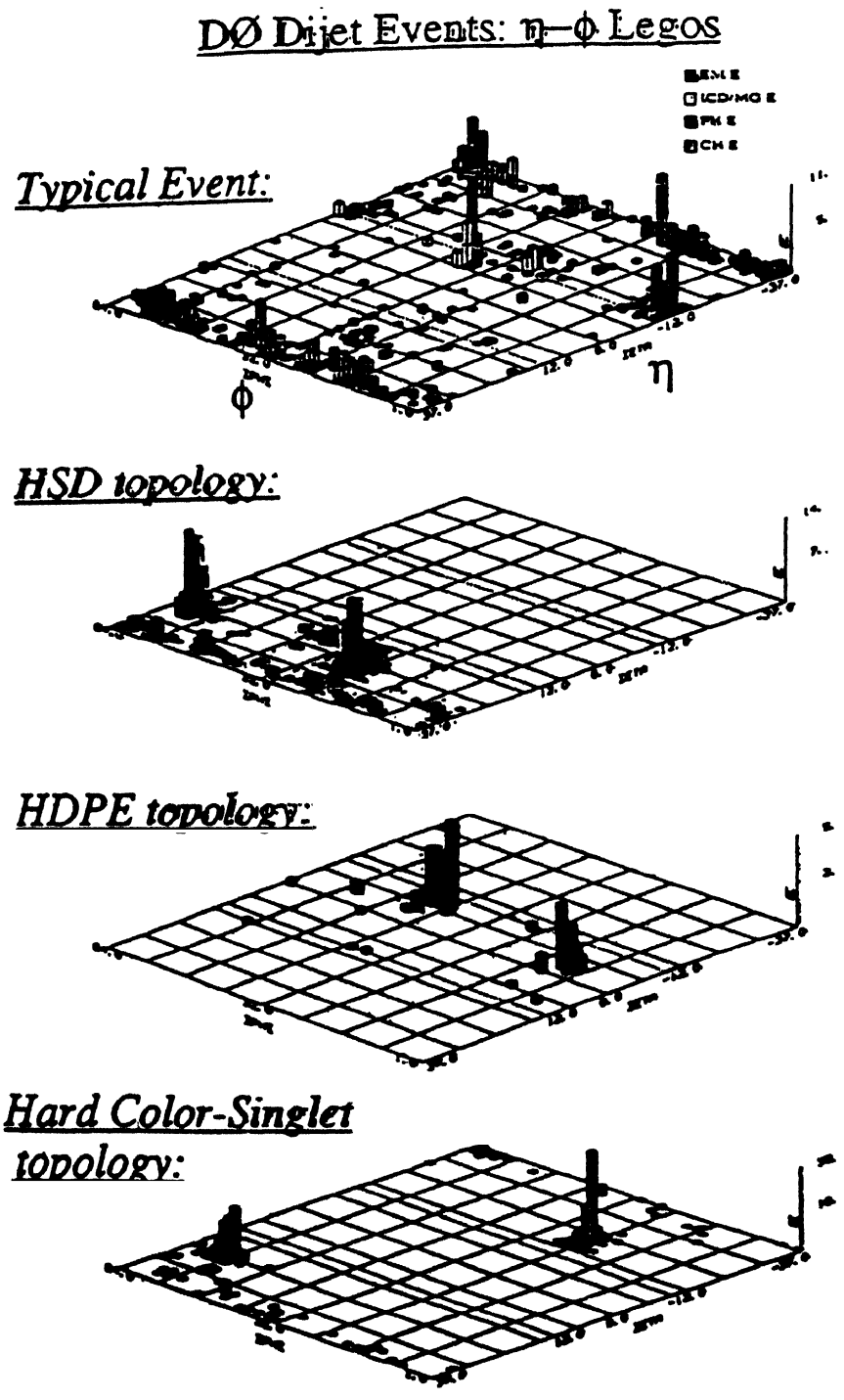

Figure 10. Lego plots of D0 dijet events in the η–ϕ plane. Note the large rapidity gap for the case of Hard Colour-singlet exchange.

possibly due to hard colour-singlet exchange is striking. There is almost nothing between the two main jets.

In order to efficiently collect data on rapidity gaps, both CDF and D0 have introduced special triggers to select events with high E_T jets with large gap in their η's. Figure 11 shows the number of EM calorimeter towers observed in D0 experiment (earlier data) [10] ($\Delta\eta \times \Delta\phi = 0.1 \times 0.1$) above a 200 MEV transverse energy threshold (n_{cal}) *versus* the number of central tracks (n_{trk}) in the region $|\eta| < 1.3$ for the (a) opposite-side and (b) same-side jet samples. The two distributions are similar in shape except at very

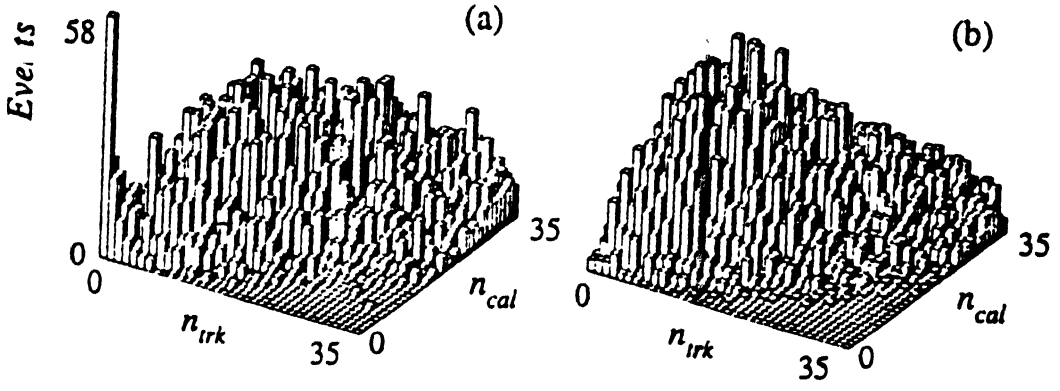

Figure 11. The calorimeter tower multiplicity (n_{cal}) in D0 experiment shown against the charged track multiplicity (n_{trk}) in the pseudorapidity region $|\eta| < 1.3$ for (a) opposite-side and (b) same-side jet samples. Only the opposite-side case shows the striking excess of events in the low multiplicity region which is typical of a colour-singlet exchange.

low multiplicities, where the opposite-side sample has a striking excess of events. The fractional excess above background is $1.07 \pm 0.10\ (\text{stat})^{+0.25}_{-0.13}$ (syst)%, which is consistent with a strongly-interacting colour-singlet (colourless) exchange process and cannot be explained by electroweak exchange alone. D0 group has subsequently reported a total of 255 candidates with rapidity gaps in the central region. CDF group also has deduced [11] similar value for the excess in the low multiplicity region from data shown in Figure 9 as evidence for colour-singlet exchange.

(ii) Dijet mass and angular distributions :

The study of dijets offers a new physics tool to study density matrix and QCD. But systematic uncertainties and energy scale have to be considered carefully before extracting physics from dijets.

The dijet mass distributions from CDF and D0 experiments [7,12] are shown in Figure 12. For the CDF figure the solid line represents a best fit to data and the boxes are the leading order QCD predictions using PYTHIA Monte Carlo. The jets produced by the Monte Carlo calculation have been smeared using the CDF detector simulation and analyzed in the same manner as the CDF data. The agreement between the data and NLO expectation is very good. Similar agreement between theory and experiment is evident in

the case of the angular distributions of the dijet events as shown in Figure 13 where the quantity $1/N\ dN/d\chi$ is plotted against the angle variable $\chi = (1 + \cos\theta^*)/(1 - \cos\theta^*)$ (θ^* = the centre of mass scattering angle).

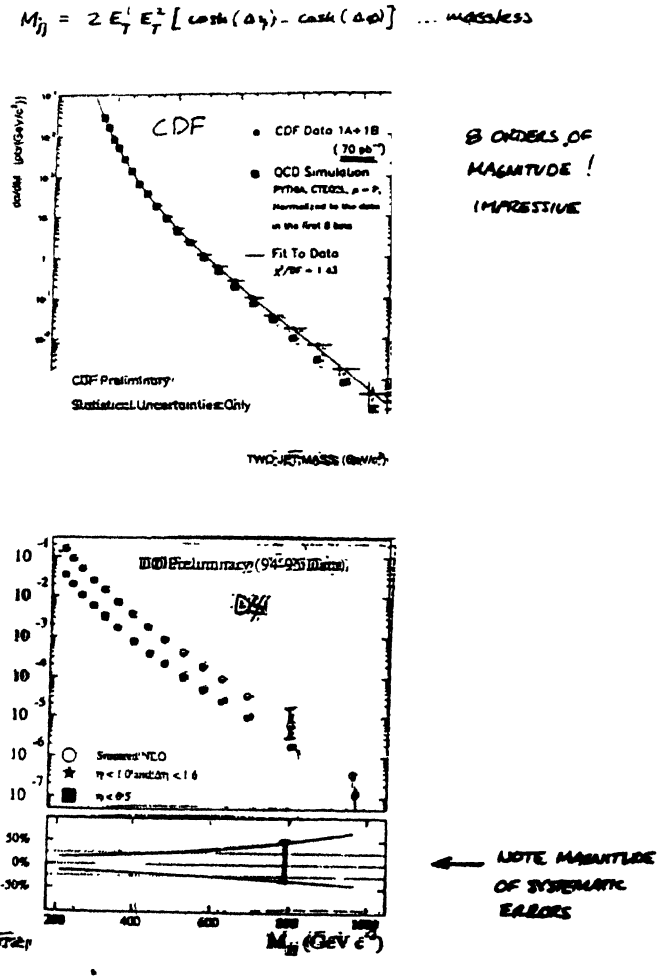

Figure 12. The results of CDF and D0 on the dijet mass distribution. The overall agreement of data with QCD simulation results using PYTHIA event generator and CTEQ2 PDF (after smearing of calculated values with detector resolution) is good.

3. Direct photon results

Prompt photon production directly probes the partonic interactions without the ambiguities associated with jet identification, fragmentation and jet energy measurement (hadronic part) as was the case with jet studies. The dominant modes of production of direct photon are from gluon-quark and quark-quark scattering, the former process making the outgoing photon a unique probe for the incoming gluon.

Direct photons are identified by the shape of an isolated shower in the central region ($|\eta| < 0.9$) inside the electromagnetic calorimeter, start of shower without a track and

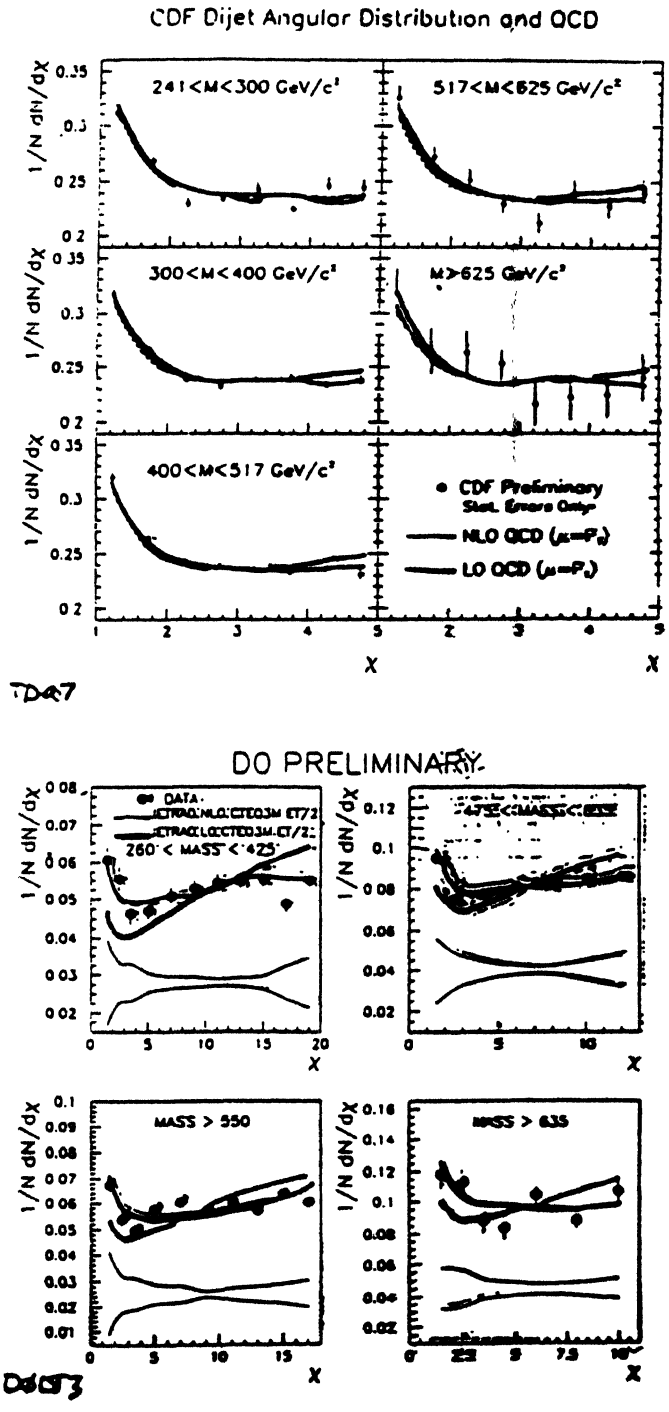

Figure 13. The angular distribution of diget events from CDF and D0 experiments. The agreement of NLO calculation and data is good.

absence of W (checked from energy measurements). Larger cuts on photon P_T increase the purity of the sample (20 GeV/c : 25% and 60 GeV/c : 80%). The direct photon inclusive

cross sections from D0 [7,13] and CDF [14] are shown in Figure 14. Overall agreement with theory is satisfactory but there is mismatch in the region below photon $P_T < 20$ GeV/c.

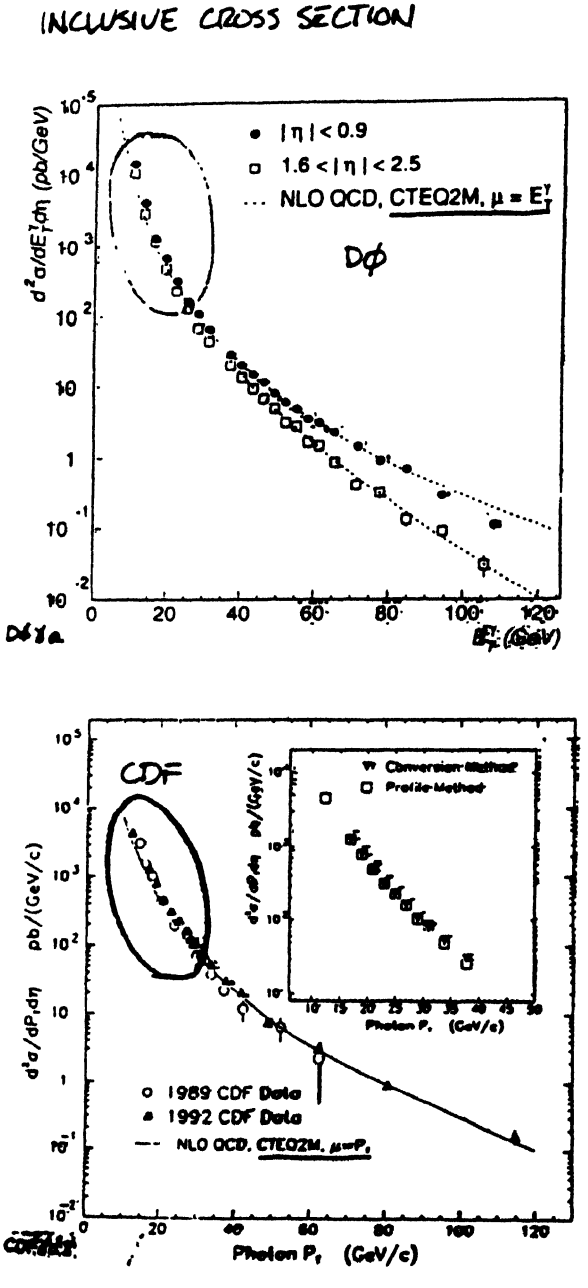

Figure 14. The direct photon inclusive cross section from CDF and D0 as a function of E_T. The results deviate from NLO model predictions for $P_T^\gamma < 20$ GeV/c.

This is more conspicuous in Figure 15 where the ratio (data-theory)/theory is shown for CDF and D0. As P_T^γ decreases the cross section seems to increase compared to the theory.

The theoretical predictions are from Baer *et al* [15] using CTEQ2M parton distributions. The theoretical calculation has been smeared with experimental energy resolution and

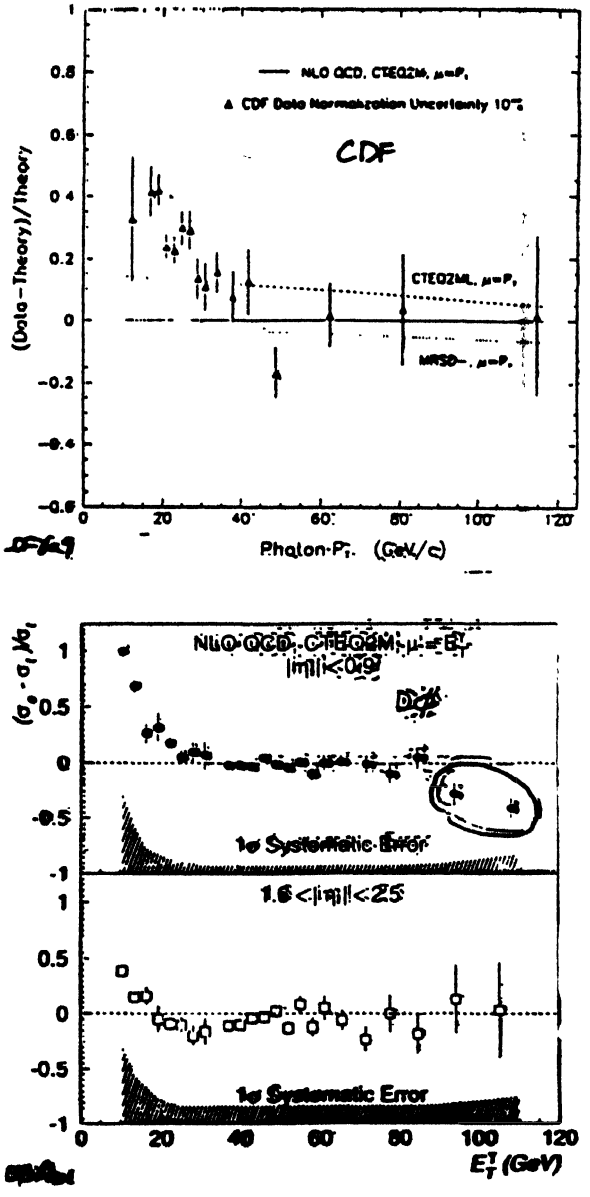

Figure 15. The ratio (data-theory)/theory for direct photon inclusive cross section shown for CDF and D0. The deviation of data from theory for $P_T^\gamma < 20$ GeV/c is notable. But systematic uncertainties are large below $P_T^\gamma < 20$ GeV/c.

includes an isolation requirement to match that applied to the data. The figure corresponding to D0 results also shows the systematic uncertainties which seem to increase as P_T^γ decreases. Because of this it is not possible to make any strong conclusion about the mismatch.

4. W + jets

Measurements of $W + n$ jets production cross sections in p-pbar interactions have gained importance due to the possibility of studying the strong interaction coupling constant (α_s) through them. In both the leading order and next-to-leading order QCD theory, one naively expects that the ratio of $W + 1$ jet and $W + 0$ jet cross sections will be proportional to the strong coupling constant. Previous experiments UA1 and UA2 at $\sqrt{s}$ = 630 GeV had used this proportionality to extract a value of α_s. The D0 experiment probes α_s at much higher centre of mass energies making the study more amenable to theory.

The process for $W + 0$ jet production does not have any strong interaction vertex and thus has no α_s dependence. On the other hand the processes for $W + 1$ jet production whether through $q\bar{q}$ or qg interactions have each 1 strong interaction vertex. So one expects, at leading order, the ratio of $W + 1$ jet to $W + 0$ jet should be proportional to α_s, neglecting any dependence on the parton distribution functions. In NLO theories, the situation is more complicated, but there is a small dependence on α_s.

In the D0 experiment for a luminosity of 83 pb^{-1} during 1994–1995 run, there were 36,891 $W \rightarrow e\nu$ candidates [16,17]. The electrons were identified by an electromagnetic fraction > 95% in the EM calorimeter shower (with $E_T > 25$ GeV) and shower shape. The electrons were required to be isolated from other objects in the event, and have a match between the calorimeter shower and a track in the central tracking detector. The W's were identified by missing E_T due to the neutrino. The backgrounds from 'QCD fakes' ($W + 0$ Jet : 1.6% and $W + 1$ Jet : 6.8% with Others : 2%) were measured without any cut on missing E_T.

The ratio

$$R_{10} = \frac{\sigma_{W+1\,\text{jet}}}{\sigma_{W+0\,\text{jet}}} \quad \frac{N_{W+1\,\text{jet}}}{N_{W+0\,\text{jet}}}$$

was surprisingly found to be [10] $0.079 \pm 0.002 \pm 0.005$ without any significant variation over an α_s region from 0.105 to 0.128 where systematic error is dominated by uncertainty in the energy scale. This is shown in Figure 16 where the NLO theoretical estimate of the ratio (using the DYRAD Monte Carlo and CTEQ3 parton distribution functions in which α_s has been varied by varying the Λ_{QCD} in the fits) is also shown. The theoretical values are well below the experimental values even after accounting for the systematic uncertainties in the measurement. Moreover, the theoretical predictions at $\sqrt{s}$ = 1800 GeV show only a slight dependence on the value of α_s. The main difference between $\sqrt{s}$ = 630 GeV and $\sqrt{s}$ = 1800 GeV is in the momentum fraction of the initial partons in the W production. The $\sqrt{s}$ = 1800 GeV data probes a much lower momentum fraction (x) region and here the gluon distribution is not well constrained and is difficult to measure. It is possible that

changes in the gluon distribution functions at low x are cancelling the effects of increasing the value of α_s.

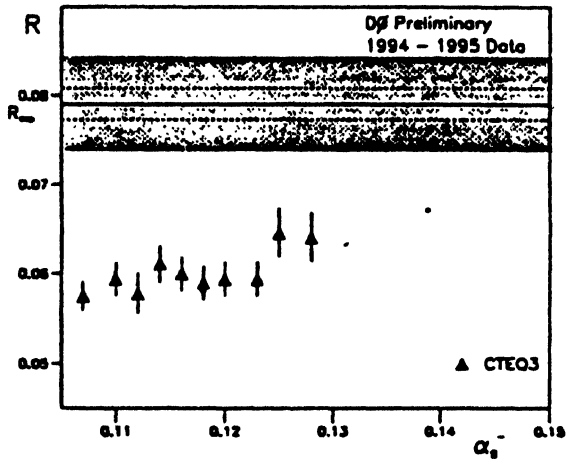

Figure 16. The ratio of W + 1 jet and W + 0 jet cross sections from D0 plotted as a function of the strong interaction coupling constant α_s. The data yields a constant value over a region of α_s from 0.105 to 0.128. The points show the results of NLO model with CTEQ3 PDF.

5. W lepton charge asymmetry

The W lepton charge asymmetry is defined as

$$A(\eta) = \frac{N_+(\eta) - N_-(\eta)}{N_+(\eta) + N_-(\eta)},$$

where $N_+(\eta)$ and $N_-(\eta)$ are the number of positrons and electrons with the same η from W^+ and W^- events respectively.

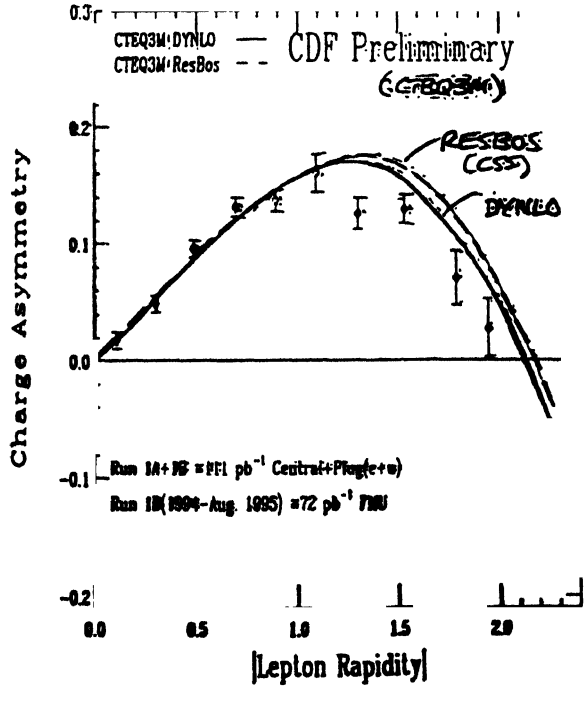

Figure 17. The CDF results on W lepton charge asymmetry as a function of the absolute value of lepton rapidity. The solid lines show the theoretical predictions of two versions (RESBOS and DYNLO) of NLO model with CTEQ3M PDF.